



Polyurethane films prepared with isophorone diisocyanate functionalized wheat starch

Reza Hosseinpourpia^{a,*}, Stergios Adamopoulos^b, Arantzazu Santamaria Echart^c, Arantxa Eceiza^d

^a Department of Forestry and Wood Technology, Linnaeus University, Lücklgs Plats 1, 35195 Växjö, Sweden

^b Department of Forest Biomaterials and Technology, Division of Wood Science and Technology, Swedish University of Agricultural Sciences, Box 7008, 750 07 Uppsala, Sweden

^c Centro de Investigação de Montanha, Instituto Politecnico de Bragança, Bragança, Portugal

^d Materials + Technologies' Group, Department of Chemical & Environmental Engineering, Polytechnic College of San Sebastian, University of the Basque Country UPV/EHU, Pza. Europa 1, 20018 Donostia-San Sebastián, Spain

ARTICLE INFO

Keywords:

Polyurethane
Wheat starch
IPDI
Isocyanate chemistry
Bio-composite films
Modification of polysaccharides

ABSTRACT

This study reports the fabrication and performance of sustainable polyurethane (PU) films based on wheat starch (native NS, modified MS), bio-polyols (1,3-propanediol PD, glycerol Gly), and polymeric diphenylmethane diisocyanate (pMDI). NS was successfully modified with isophorone diisocyanate, confirmed by Fourier transform infrared spectroscopy (FTIR) and ¹³C nuclear magnetic resonance (¹³C NMR). Various PU films were prepared using NS, PD or Gly, MS and pMDI. For comparison, reference films were also synthesized without MS. PU films were analyzed from the viewpoint of their chemical, thermomechanical and flexural properties, and microstructural morphology. FTIR spectra demonstrated the total consumption of NCO groups, while the scanning electron microscopy micrographs of the films revealed that MS addition promoted the interactions between the compounds, enhancing in consequence their mechanical and thermomechanical performance. The study supported the suitability of functionalized carbohydrates to substitute petrochemical compounds in the synthesis of more environmentally-friendly PUs.

1. Introduction

Polyurethane (PU) is one of the commonly used materials in automotive, building and construction, electronics, sportswear, and packaging industries due to its structure and versatile properties [1]. The nature, performance and application of PUs depend on the chemical structure of the starting reactants, that is, the diisocyanate/polyisocyanate, with –NCO functional groups and –OH terminated oligomer, polyol [2]. Thermoplastic PUs are formed through the reaction of a diisocyanate and a bi-functional polyol that leads to a PU with relatively poor mechanical properties in comparison with thermoset PUs, where the introduction of a precursor/crosslinker with more than two functional groups result in PUs with improved physical and mechanical properties [2,3].

Preparation of PUs from renewable sources has received considerable attention during the last decade due to economic and environmental concerns [4]. Vegetable oil, lignin, and cellulose nanoparticles

were the most studied biomaterials in PU synthesis [1,5–8], whereas there are few works highlighting the use of starch for PU preparation. Starch, as one of the most widely available carbohydrates, is an attractive biopolymer for various applications including food, textile, pharmaceutical, paper, and biofuel industries [9]. This co-polymer consists of two macromolecular complexes, amylose and amylopectin [10]. The proportion of each component varies not only from the species, but also within a given plant [11], and it affects the performance of starch, especially its water holding capacity [12]. In PU composites, starch acts either as a composite filler or as a –OH group provider to form covalent linkages with –NCO groups of the isocyanate matrices [2,13]. Zou et al. [14] reported the reinforcement role of starch nanocrystals in PU composites providing a considerable enhancement in both, strength and Young's modulus properties. Incorporation of gelatinized corn starch with high amylose content in PU composite film improved its hydrophobicity and mechanical properties due to the formation of urethane linkages [15]. Composite film prepared with starch, diethylene glycol,

* Corresponding author.

E-mail address: reza.hosseinpourpia@lnu.se (R. Hosseinpourpia).

<https://doi.org/10.1016/j.eurpolymj.2021.110826>

Received 11 June 2021; Received in revised form 24 September 2021; Accepted 9 October 2021

Available online 12 October 2021

0014-3057/© 2021 The Author(s). Published by Elsevier Ltd. This is an open access article under the CC BY license (<http://creativecommons.org/licenses/by/4.0/>).

and 2,4-toluene diisocyanate improved the flexible behavior, which results in a decreased tensile strength and an increased elongation at break [16]. The authors claimed that the branched structure of starch hindered its crosslinking capacity with the isocyanate, thus the diethylene glycol with linear structure reacted faster to form polyurethane linkages.

Chemical modification of starch causes distinct changes in the properties of the ensuing polymer, improves its hydrophobicity and thermal stability, and enhances its compatibility with the matrix polymer. For instance, the modification of starch nanoparticles with 1,4-hexamethylene diisocyanate (HMDI) resulted in crosslinked hydrophobic particles with enhanced thermal stability [17]. These nanoparticles were then used to enhance the electrical conductivity of the polyether-polyurethane matrix. Santayanon et al. [18] quoted that starch acetylation increased its interfacial adhesion with thermoplastic polyurethanes, enhancing, in consequence, the mechanical strength of the PU composites.

Pea starch and dextrin polymers were successfully modified with isophorone diisocyanate (IPDI) monomer in our group [19], and the obtained polymers showed higher thermal stability and hydrophobicity as compared to the unmodified counterparts. The presence of dual functionalities in starch and dextrin were also confirmed by the existence of urethane linkages and pendant isocyanate groups. The existing free isocyanate groups were expected to be available as reacting points for further reaction with additional monomers of interest. Therefore, this study hypothesizes that the functionalized wheat starch with IPDI monomer can be used, as a tuned bio-based component, for the proportional replacement of polymeric diphenylmethane diisocyanate (pMDI) in PU-based composites. Therefore, native wheat starch was firstly functionalized with IPDI monomer at NCO:OH molar ratio of 6:1 in the presence of dibutyltin dilaurate (DBTDL) as a reaction catalyst and its chemical, thermal, and morphological characteristics were compared with that of native wheat starch. Subsequently, different combinations of modified wheat starch were used together with pMDI as –NCO donor, and native wheat starch and two polyol types (1,3-propanediol and glycerol) as –OH donors, to prepare PU films. The obtained PU films were also studied for their thermomechanical, mechanical, and microstructural properties.

2. Experimental

2.1. Materials

Native wheat starch (NS), consisting of about 22% amylose and 78% amylopectine, was kindly provided by Lantmännen (>95%, Stockholm, Sweden). The functionalization of NS was carried out using isophorone diisocyanate IPDI (>99.5%, Desmodur I®, kindly provided by Covestro, Leverkusen, Germany), with a –NCO content of 37.8% and dibutyltin dilaurate DBTDL (>95%, Sigma Aldrich, Saint Louis, MO, USA) as catalyst. HPLC grade anhydrous dimethyl sulfoxide (DMSO) (>99.8%, Macron Fine Chemicals, Paris, KY, USA) was used as the starch solvent. HPLC grade toluene (>99.8%, Lab-Scan Analytical Sciences, Gliwice, Poland) and tetrahydrofuran THF (>99.8%, Macron Fine Chemicals) were used to remove the unreacted excess IPDI after modification.

Polymeric-methylene diphenyl-diisocyanate pMDI (>99.5%, Desmodur 44V20L) was kindly provided by Covestro (Leverkusen, Germany). Two polyols, 1,3-propanediol PD (bio-PDO, Susterra®, DuPont Tate & Lyle Bio Products Co, Loudon, TN, USA) and glycerol Gly (vegetable origin for analysis EMSURE® ACS, Reag. Ph Eur, Sigma Aldrich, Saint Louis, MO, USA) were used to prepare the PU films.

2.2. Functionalization of native wheat starch

NS was functionalized with IPDI according to our previous work [19]. Briefly, a 10% (wt/wt) wheat starch solution was prepared in DMSO at 90 °C. The IPDI was heated to 60 °C under a nitrogen

atmosphere in a 3-neck flask partially submerged in an oil bath. DBTDL (0.1% wt/wt) was added and stirred for 5 min. The starch solution was then added dropwise to the IPDI/DBTDL mixture with a funnel while maintaining vigorous stirring. The reaction proceeded in IPDI excess (NCO:OH molar ratio of 6:1) at 60 °C for 24 h with N₂ inlet. The reaction was halted by THF addition. The resultant mixture was centrifuged three times at 4500 rpm for 10 min (replacing the supernatant with fresh THF) to remove the DMSO and THF. The purification of the unreacted IPDI was conducted by the precipitation of the starch in toluene through three centrifugation cycles at 4500 rpm for 10 min (replacing the toluene with a fresh one per cycle). Finally, the modified wheat starch (MS) was dried in a vacuum oven at 40 °C for 48 h, and stored in a tight bottle to protect from humidity.

2.3. Preparation of PU films

A series of polyurethane films were produced according to diverse compositions including pMDI (29.8% NCO, 141 g/eq) and MS (3% NCO, 1400 g/eq) (NCO donors) and NS (31 mg KOH/g, 1809 g/eq), PD (38.0 g/eq) and Gly (30.7 g/eq) (OH donors). The NCO content (%) and OH index (mg KOH/g) in the respective polymers was determined by the titration method, according to ASTM D 2572-97 and ASTM D 4274-05 standards, respectively. According to these results, diverse compositions were defined based on the NCO:OH molar ratio of 1:1, and the formulations are summarized in Table 1. In order to maximize the usage of NS, it was considered as a polyol in the formulations. Oven-dried (vacuum oven at 40 °C for 48 h) NS was magnetically stirred with the other polyols (e.g. PD or Gly) for 3 min, and then MS and pMDI were added to the mixture and allowed to magnetically stir for 2 min. For comparative purposes, two reference formulations without MS were also prepared for each polyol series. The high viscose paste-shape mixtures were poured in a mold using a glass rod and formed under compression of a hydraulic press at 150 °C for 30 min. The produced films were stored in a tight bottle before characterization.

2.4. Characterization

The NS and MS samples were characterized by elemental analysis (EA), Fourier transform infrared spectroscopy (FTIR), ¹³C nuclear magnetic resonance spectroscopy (¹³C NMR), thermogravimetric analysis (TGA), differential scanning calorimetry (DSC), and scanning electron microscopy (SEM) while the PU films were analyzed by FTIR, dynamic mechanical analysis (DMA), flexural bending strength, and SEM techniques.

2.4.1. Elemental analysis

The carbon, hydrogen, oxygen and nitrogen contents of NS and MS were determined by elemental analysis using an EuroVector EA 3000 atomic absorption spectrometer (Pavia, Italy) heated at 980 °C with a constant flow of helium. The degree of substitution (DS) was calculated according to the methodology described by Hosseinpourpia and co-workers [19].

Table 1
Formulations of the PU films based on the NCO:OH molar ratio of 1:1.

Formulation	NS (wt. %)	Polyol (wt. %)	MS (wt. %)	pMDI (wt. %)
NS-PD-pMDI	35	13	–	52
NS-PD-MS1-pMDI	27	12	21	40
NS-PD-MS2-pMDI	25	10	29	36
NS-Gly-pMDI	35	11	–	54
NS-Gly-MS1-pMDI	28	9	22	41
NS-Gly-MS2-pMDI	26	8	30	36

* MS1 and MS2 represent lower and higher load of modified wheat starch, respectively. NS: native wheat starch, MS: modified starch, PD: 1,3-propanediol, Gly: glycerol.

2.4.2. Fourier transform infrared spectroscopy

The chemical structure of NS and MS as well as the PU films was analyzed by FTIR spectroscopy using a Nicolet-Nexus, Waltham, MA, USA equipment with a MKII Golden Gate accessory (Specac, Orpington, UK) and a diamond crystal at a nominal incidence angle of 45° and ZnSe lens. The analyses were conducted in attenuated reflection (ATR) mode, and evaluated between 4000 and 650 cm^{-1} at room temperature, averaging 64 scans with a resolution of 4 cm^{-1} .

2.4.3. ^{13}C nuclear magnetic resonance spectroscopy

The modification of wheat starch was confirmed by solid-state ^{13}C NMR using a Bruker Avance III 400 MHz equipment (Billerica, MA, USA). The spectra were recorded using a decoupled sequence at ^{13}C frequency of 100.6338 MHz at 25 °C. Samples were measured at a spinning rate of 10,000 Hz averaging 4096 scans with a recycling delay of 10 s. A time domain of 2 K was employed with a spectral width of 30 KHz.

2.4.4. Differential scanning calorimetry

The glass transition temperature (T_g) of NS and MS were recorded with a DSC analyzer (Mettler Toledo DSC3+ equipment, Columbus, OH, USA). For each sample, approximately 5 mg were subjected from -50 to 200 °C at a heating rate of 20 °C min^{-1} under a nitrogen flow of 10 mL min^{-1} .

2.4.5. Thermogravimetric analysis

The thermal stability of NS and MS was analyzed using a Q500 TA equipment (New Castle, DE, USA). Around 5 mg of each sample were heated from 25 to 750 °C at a rate of 10 °C min^{-1} , under a nitrogen atmosphere.

2.4.6. Dynamic mechanical analysis

The thermomechanical properties of the PU films were characterized by DMA, GABO Eplexor 100 N from Netzsch-Gerätebau GmbH (Selb, Germany), in strain mode, with a preload of 0.8 N and a static strain of 2% and a dynamic strain of 0.5%. The bending performances of the composite films were determined using a constant frequency of 1 Hz, temperature range from 25 to 250 °C and heating ramp of 3 °C min^{-1} . The sample dimensions were 36 mm in length, 12 mm in width and 1.8 mm in thickness using a span of 20 mm.

2.4.7. Flexural bending strength

The flexural strength of the PU films was characterized by a three-point bending test using an Instron 5967-30kN testing machine at a load rate of 2 mm min^{-1} . The dimension of samples was 36 mm in length, 12 mm in width and 1.8 mm in thickness. A one-way analysis of variance (ANOVA) was performed on the flexural strength results with SPSS version 25.0 statistical software package (IBM Corp., Armonk, NY, USA). Statistical differences between the values were assessed by Tukey's honestly significant difference (HSD) test at an error probability of $\alpha = 0.05$, as previously described [20].

2.4.8. Scanning electron microscopy

The morphology of NS and MS, and the fractured surfaces of PU films after flexural strength testing were characterized by SEM. A JEOL JSM-7000F equipment (Akishima, Japan) was used operating at 20 kV with a surrounding beam current between 0.01 and 0.1 nA to obtain secondary electron images. Dried samples were placed over a double-sided carbon-based conductive tape and covered with a 20 nm Au in order to make the surface conductive.

3. Results and discussion

3.1. Characterization of NS and MS

The content of C, H, N, and O elements in NS and MS samples was

analyzed by EA and the results are summarized in Table 2. A negligible content of nitrogen was found in NS, while MS demonstrated to hold considerable amounts of nitrogen, indicating that the IPDI was present. The content of nitrogen in MS was found to be relatively higher than the one reported previously for pea starch at a comparable modification condition [19].

The extent of modification is described by the degree of substitution, DS [1]. The results of the elemental analysis were used to calculate the DS for MS. Each anhydroglucose unit of the starch macromolecule has three -OH groups at C₂, C₃ and C₆ available for substitution with one IPDI monomer, making a total theoretical degree of substitution (DS_{total}) of 3.0 [21]. The -OH group on the primary carbon (C₆) is more reactive than the secondary ones on C₂ and C₃. The reactivity of -OH group on C₂ is also slightly higher than the C₃, mainly due to its vicinity to the hemiacetal group [22]. To determine the level of -OH group participation for modification of wheat starch with IPDI, the modification efficiency (ME) was then calculated by considering the DS and DS_{total} values. To reach the theoretical DS_{total} value, the resulting DS varies between 0 and 3, which results in an ME variation between 0 and 1. MS indicated an ME value of 0.49, which was about two times higher than the one reported previously for modified pea starch, i.e. modified pea starch at comparable NCO:OH ratio showed DS value of 0.77 that corresponds to ME value of ~ 0.25 [19]. This value implies that nearly half of the available -OH groups in the glucosidic unit of the starch polymer were substituted with the -NCO groups. More detailed information regarding the calculation of DS and ME can be found in the Supplementary Materials.

The changes in the chemical structure of NS after modification with IPDI was analyzed by means of FTIR and solid ^{13}C NMR spectroscopies (Fig. 1a,b). The FTIR spectra (Fig. 1a) showed a vibration in NS and MS at a range of 3250 cm^{-1} to 3450 cm^{-1} . This absorption in NS is mainly assigned to the stretching of the -OH groups, however, after modification with IPDI these peaks were decreased, which indicates many of these -OH groups were consumed and also urethanes linkage (NH bonds) were formed between isocyanate and alcohol groups. The latter led vibration at about 3390 cm^{-1} in MS. Both NS and MS illustrated a stretching vibration at 2960 cm^{-1} , which is attributed to the carbon-hydrogen bond [23]. NS exhibited two absorption peaks at 1000 and 1200 cm^{-1} , which are assigned to the carbon-oxygen stretching of the polysaccharide skeleton. These absorption peaks were apparently decreased in MS. The appearance of the new peaks at 2266 cm^{-1} , 1750 cm^{-1} , 1530 cm^{-1} , and 1250 cm^{-1} , which are respectively related to the pendant -NCO groups, carbonyl group, and amino and cyanide groups, confirmed that the starch polymer was successfully functionalized with the IPDI monomer [1,7,19].

Solid-state ^{13}C NMR spectroscopy illustrated the obvious changes in the chemical structure of starch polymer after modification with IPDI (Fig. 1b). The signal at 61.8 ppm in NS is related to glycosidic C₆ [24], while the overlapping peaks at around 68–78 ppm were attributed to the carbons C₂, C₃ and C₅. The carbons C₁ and C₄ showed their respective resonances at 81.1 and 100.7 ppm. These signals were slightly different as compared with the ones reported previously for unmodified pea starch and dextrin, which might be due to the sensitivity of these carbons to chain conformations [19,25]. MS showed new signals in the regions between 20 and 50 ppm that were related to the hydrocarbons presented in IPDI, i.e. CH₃ peaks at $\delta = 23.5$ and 27.8 ppm, CH₂ peak in the aliphatic part of IPDI at $\delta = 45.2$ ppm, and signals of CH at $\delta = 26.9$ and 32.3 ppm [1,7]. The new peaks in $\delta = 123$ –129 ppm and $\delta =$

Table 2
Elemental composition of NS and MS polymers, and modification efficiency (ME).

Type of Starch	C	H	N	O	ME
NS (wt %)	39.3	6.8	<1.6	38.5	–
MS (wt %)	56.5	8.4	8.0	20.1	0.49

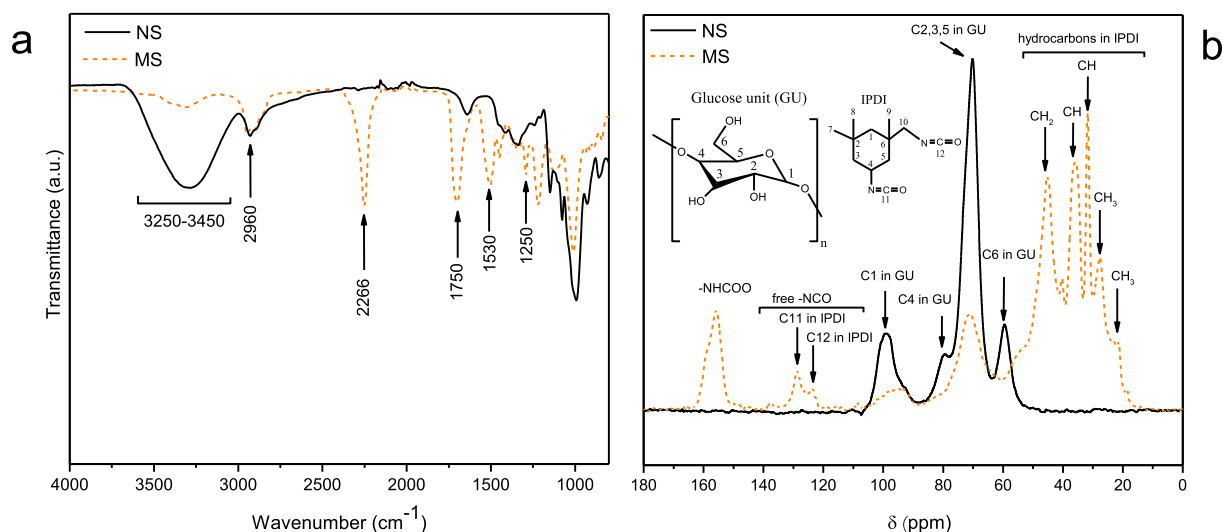


Fig. 1. FTIR spectroscopy (a) and ^{13}C NMR spectra (b) of NS and MS polymers.

155–157 ppm were attributed to free $-\text{NCO}$ groups and urethane linkages, respectively. Two distinct peaks were observed at $\delta = 123.59$ and 128.64 . As reported previously by Girouard et al. [1], signals related to primary and secondary isocyanates in solid-state ^{13}C NMR shift slightly as compared with liquid NMR, and thus in solid-state ^{13}C NMR the peak at ~ 124 ppm corresponds to the primary isocyanate, and the peak at ~ 129 ppm relates to the secondary isocyanate. The secondary isocyanate generally shows higher absorption than the primary one [1,19]. The reaction between the secondary $-\text{NCO}$ group from IPDI and the $-\text{OH}$ groups from starch polymer was evidenced by the appearance of a new peak corresponding to urethane linkages at 155.87 [26,27]. These results, together with FTIR and elemental analysis, confirmed that the MS has both urethane and isocyanate functionalities. In addition, the presence of available primary and secondary $-\text{NCO}$ groups make MS a suitable component in the preparation of PU films or composites.

Thermal degradation of the oven-dried NS and MS samples was examined by thermogravimetric (TG) and first derivative thermogravimetric (DTG) analyses (Fig. 2a). NS began to lose weight below 100°C , which might be due to the water molecules bounded in the granule structure of NS. The moisture sorption capability of NS was most likely decreased after modification with IPDI (Supplementary Materials), and thus such a weight loss was not apparent in MS. The DTG curve was derived from the TG graph and exhibited a maximum degradation

temperature at 313°C for NS that is associated with its thermal decomposition [19,28]. Functionalization of NS with IPDI considerably changed the degradation pattern as MS shifted the degradation temperature to approx. 23°C higher at $\sim 335^\circ\text{C}$. The second maximum degradation temperature occurred at $\sim 416^\circ\text{C}$, related with the IPDI attached to the starch backbone. These results are in agreement with the previous studies on thermal degradation analyses of cellulose nanocrystals, kraft lignin, and pea starch and dextrin after functionalization with IPDI [1,19,26].

The effect of functionalization of NS with IPDI on the glass transition temperature (T_g), after removing the first thermal history of the oven-dried samples, are presented in Fig. 2b. The NS showed a T_g at 147.6°C , while the T_g was shifted in MS to 99.7°C . Noticeable decreases in T_g of kraft lignin, pea starch and dextrin by modification with IPDI were also reported previously [19,26]. The decrease in T_g of MS could be due to the replacement of $-\text{OH}$ groups in the glucoside unities of starch with $-\text{NCO}$ groups and the formation of urethane linkages instead of hydrogen bonds, which increases the mobility of the polymer [29]. Also, the existence of the suspended primary and secondary $-\text{NCO}$ groups on the starch backbone may impede the packaging ability of the polymer due to steric hindrance, and thus decrease the T_g [19].

Fig. 3a and b show the SEM micrographs of starch granules before and after modification. The granular structure of starch and the size of

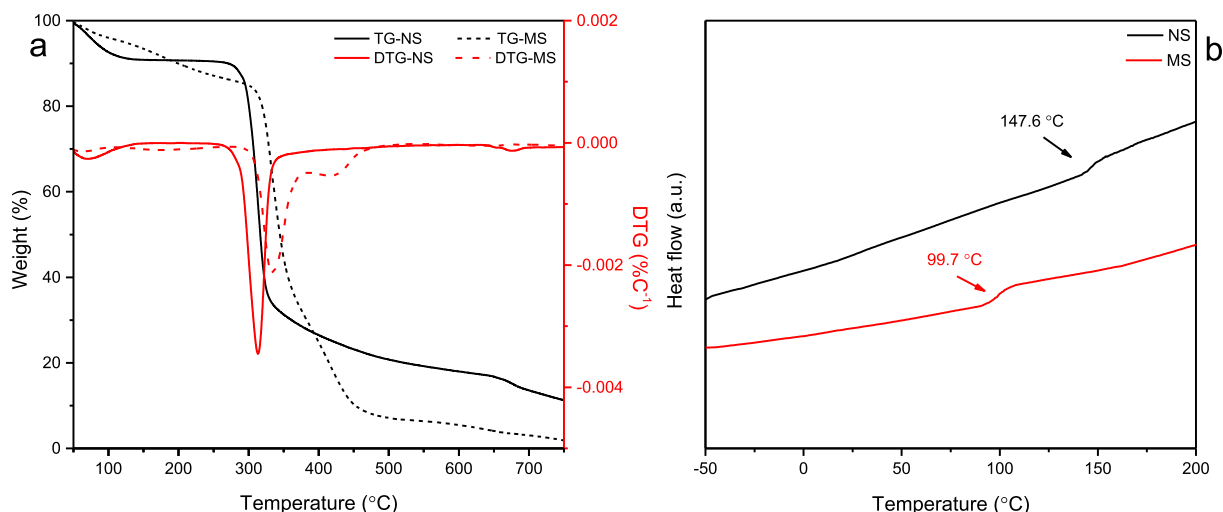


Fig. 2. Weight changes and DTG (a) and DSC thermographs (b) of NS and MS polymers.

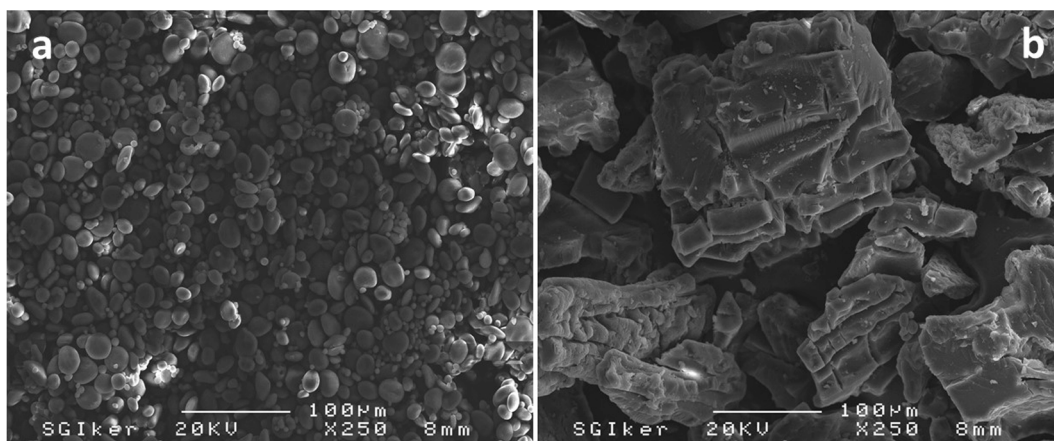


Fig. 3. SEM micrographs of NS (a) and MS (b) granules.

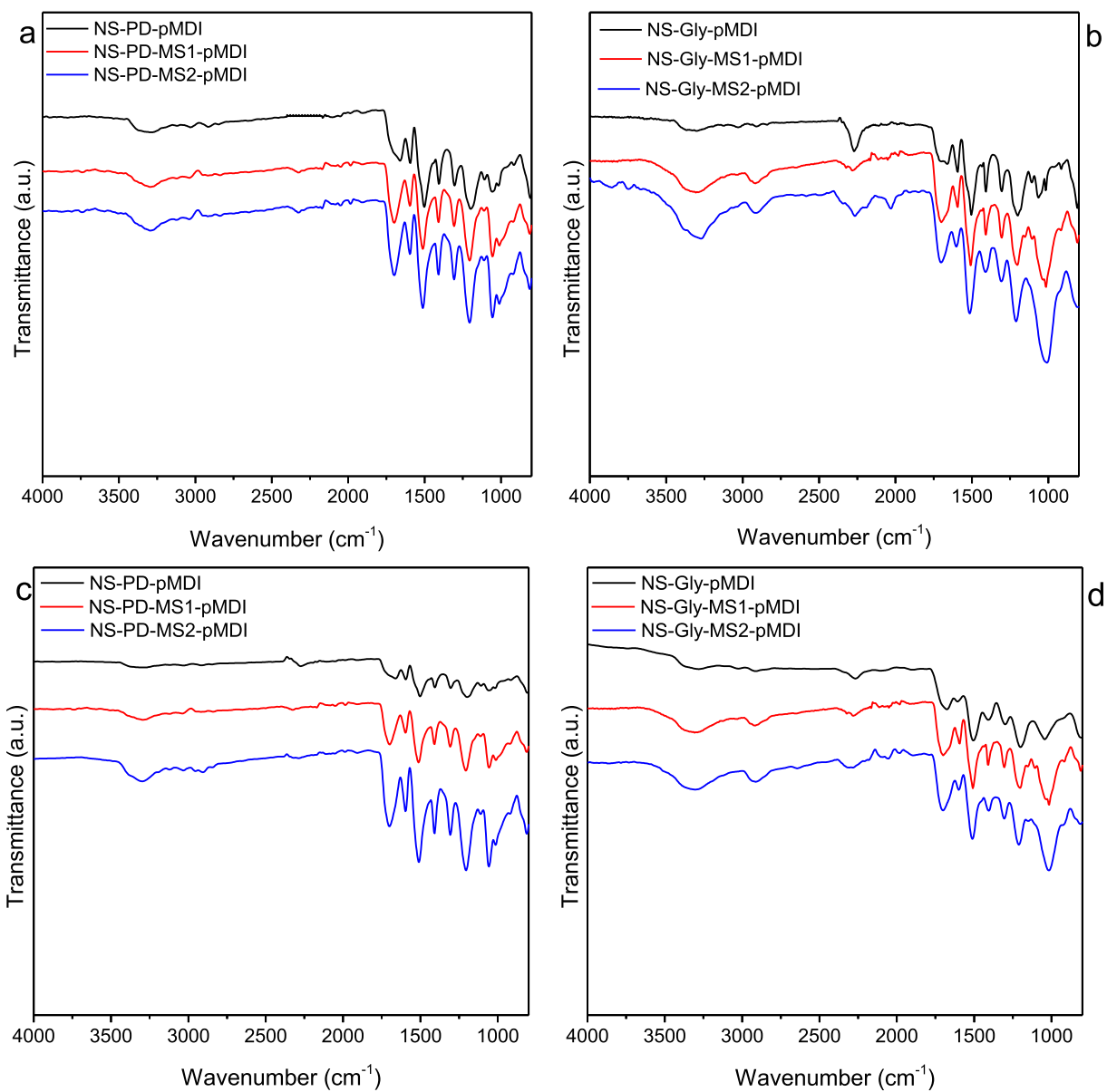


Fig. 4. FTIR spectroscopy of PU films after molding (a, b) and after post-curing (c, d).

the granules were changed obviously due to IPDI functionalization. This result is in agreement with the previous reports [19,29]. Hosseinpourpia and coworkers [19] described that the excess amount of IPDI in the reaction could cause side reactions between its primary $-NCO$ groups and $-OH$ groups of starch, which resulted in increased granule size and intra-connection of granules. The SEM micrographs together with the previous chemical, thermal and sorption analyses, confirmed the successful modification of wheat starch polymer with IPDI monomer.

3.2. Characterization of PU films

The NS and MS particles were incorporated in the preparation of PU films using a diol or triol and pMDI according to the method outlined in the Materials and methods section. The chemical, thermomechanical and mechanical properties and microstructural characteristics of the PU films were assessed with FTIR, DMA and flexural bending, and SEM, respectively.

FTIR spectroscopy was used to monitor the chemical structure of PU films as a function of their components (Fig. 4a-d). There were no obvious differences in the FTIR spectra of the PU films that contained NS and/or MS. The wide vibration at 3450 cm^{-1} was attributed to the $-OH$ groups in the starch polymers and also the $N-H$ bond in the urethane group. The stretching vibration at 2266 cm^{-1} , which is assigned to the free $-NCO$ groups, disappeared in the PU films containing PD (Fig. 4a). However, the films with Gly showed slight vibration at 2266 cm^{-1} indicating that the free $-NCO$ groups were not entirely consumed (Fig. 4b). It seems that higher energy is required for the triol (Gly) than the diol (PD) to complete the reaction with $-NCO$ groups. Therefore, a post-curing step was applied for all films at $160\text{ }^{\circ}\text{C}$ for 30 min. The FTIR spectra of the PU films after the post-curing step exhibited that the peak

related to free $-NCO$ groups at 2266 cm^{-1} disappeared, evidencing that these functional groups were consumed (Fig. 4c,d). This fact, together with an apparent decrease at the range of $3250\text{--}3450\text{ cm}^{-1}$, confirmed that the reaction between the $-OH$ groups in NS and polyol with the $-NCO$ groups in MS and pMDI was completed and also the NH bond was formed. The peaks at 1750 and 1530 cm^{-1} were assigned to urethane bonds. These vibrations together with the peaks in the fingerprint region between 1500 and 800 cm^{-1} , which attributed to the ether, amine, and hydrocarbon bonds in the polysaccharide skeleton and pMDI polymers (Girouard et al., 2016), were identical for all films. The FTIR spectra illustrated a similar chemical structure and vibration of urethane linkages in all PU films.

The dynamic thermomechanical behavior for the post-cured PU films as a function of polyols and MS are shown in Fig. 5a-d. The NS-PD-pMDI film exhibited slightly higher storage modulus (E') than the NS-Gly-pMDI at $25\text{ }^{\circ}\text{C}$. The E' of the films increased by increasing the MS content during the entire temperature range, which could be due to the formation of a highly crosslinked network as a result of the replacement of pMDI by MS, with more functionalities (both OH and NCO). The E' of the films decreased slowly with increasing the temperature from $25\text{ }^{\circ}\text{C}$ to $60\text{ }^{\circ}\text{C}$. The slope of E' curves were identical for both polyol types up to about $60\text{ }^{\circ}\text{C}$, which implies a similar behavior at the low temperatures. With increasing the temperatures at above $60\text{ }^{\circ}\text{C}$, the films with PD polyol illustrated a drastic decrease in storage modulus (Fig. 5a), while a progressive E' decrease was observed in the films contain Gly polyol (Fig. 5b). The highest E' was observed in the film with NS-Gly-MS1-pMDI. The loss modulus (E'') of composites is correlated with the nature of polymer materials and the ability of the materials to dissipate energy by internal friction and molecular motions [30,31]. As the temperature increased a drastic drop point in E' curve was observed, at

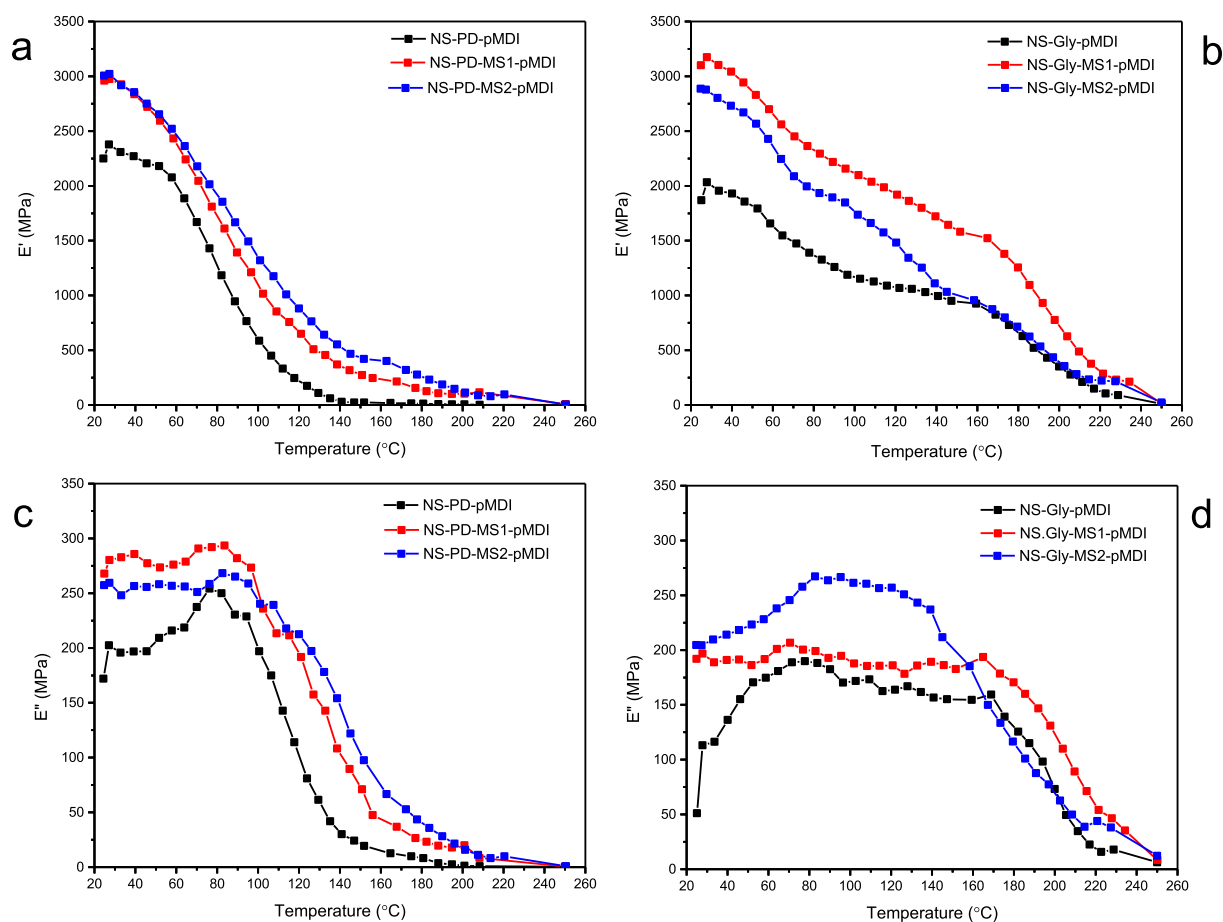


Fig. 5. Storage modulus (E') (a,b) and loss modulus (E'') (c,d) of PU films.

the same time that presents an E'' maximum, which associated with the glass transition temperature, T_g . As shown in Fig. 5c and d, the E'' and T_g of PU films changed considerably because of the polyol types and the added MS. The films with Gly polyol exhibited a wide transition in E'' curves at elevated temperatures as compared with the peak-like pattern in PD containing films. This could be attributed to the relaxation of different heterogeneous crosslinked points between NS and MS with pMDI or between Gly with MS and pMDI. The T_g for NS-PD-pMDI was 82.2 °C while for the NS-Gly-pMDI film was at 168.9 °C, which is related to the contribution of the trifunctional molecule, Gly, in crosslinking reactions [32]. The E'' maximum increased in the PU films by replacement of pMDI with MS. The average functionality of standard pMDI is between two to three [33]. Replacing the pMDI by MS with more functionality (due to the existence of both –OH and –NCO groups in the anhydroglucose unit of MS) could enhance the crosslinking density, and thus lead to the higher thermomechanical strength. In the films with PD polyol, the T_g increased by increasing the MS content, suggesting that the energy dissipation is shifted to the higher temperatures by increasing the MS content. Although the E'' of the films that contained Gly increased by MS, the T_g slightly decreased by increasing the MS content, which is attributed to the reduction of Gly content. The dynamic thermomechanical analysis of the PU films showed that the PU films prepared with less pMDI even could bear higher stress, due to the enhanced crosslinking density.

The flexural bending properties of the post-cured PU films with different polyols and MS contents are shown in Fig. 6a and b. The films composed of NS and Gly (NS-Gly-pMDI), had a statistically significant higher flexural strength than that of films with NS and PD polyol (NS-PD-pMDI) (Fig. 6a, ANOVA, $\alpha = 0.05$), which could be attributed to the higher crosslinking density of the films with Gly polyol. MS considerably contributed to the improvement of films' strengths. This agrees with the E' values measured by DMA (Fig. 5a and b). The bending strengths of the films were noticeably increased with increasing the content of MS. Differences were statistically significant in all PU films, except for NS-Gly-MS2-pMDI (ANOVA, $\alpha = 0.05$). For the films with PD polyol, the highest bending strength value was obtained from the NS-PD-MS2-pMDI film, while NS-Gly-MS1-pMDI exhibited the highest value among the films that included Gly. This result is in agreement with the one from the dynamic thermomechanical analysis. The Young's moduli of the PU films are presented in Fig. 6b, and illustrated the elasticity of the films that could reach infinity for a perfectly rigid material [34]. The Young's modulus increased by adding MS and also by increasing the MS content. The NS-Gly-MS2-pMDI film exhibited the highest Young's modulus with a value of 3430 MPa. As observed in flexural bending strength, the slightly higher value observed in NS-Gly-MS2-pMDI in comparison to NS-Gly-MS1-pMDI could be related to the higher stiffness of the film as a

result of a highly crosslinked network.

3.3. SEM of PU films

SEM micrographs from the fractured surfaces of PU films after flexural tests are presented in Fig. 7a-d. It was observed that NS granules acted as a flaw in the PU films (Fig. 7a and c). This was more pronounced in the composition with PD polyol (NS-PD-pMDI), while relatively higher interaction between NS and the surrounding matrix was observed in the film containing Gly. The cracks might have been created at the interfaces of the NS granules, particularly in the films containing PD polyol, during the test due to the increasing molecular weight between the crosslinking points, which resulted in a reduction of the flexural strength of the PU films. This finding supports the results from the dynamic thermomechanical and flexural analyses. The addition of MS improved the interactions between NS, polyols and pMDI (Fig. 7b and d). Considerably high compatibility was observed in the films with a higher level of MS (NS-PD-MS2-pMDI, NS-Gly-MS2-pMDI), as the granules of NS were hardly detectable. More images from the fractured surfaces of the PU films with low MS content are given in the Supplementary Materials.

4. Conclusions

NS was successfully functionalized with IPDI at a NCO:OH molar ratio of 6:1 in the presence of DBTDL, as a reaction catalyst. The existence of urethane linkage and pendant isocyanate groups on the MS polymer was confirmed by FTIR and ^{13}C NMR analysis. The MS was then used together with NS and PD or Gly for the partial replacement of synthetic pMDI in the synthesis of PU films, at NCO:OH molar ratio of 1:1. FTIR spectroscopy showed that higher energy was needed for the films with Gly to complete the reaction between –NCO groups of pMDI and MS, and –OH groups of NS and polyols. The dynamic thermomechanical, flexural bending and SEM analyses showed that the replacement of pMDI by MS enhanced the crosslinking density between the precursors, which resulted in a considerable improvement of the mechanical strength properties. This study demonstrated the high-performance PU films can be manufactured with IPDI modified wheat starch to reduce the levels of pMDI in the polymer, thus offering an innovative strategy to overcome the challenge of formulating high strength PU elastomers through sustainable approaches for a wide range of applications.

CRediT authorship contribution statement

Reza Hosseinpourpia: Conceptualization, Funding acquisition,

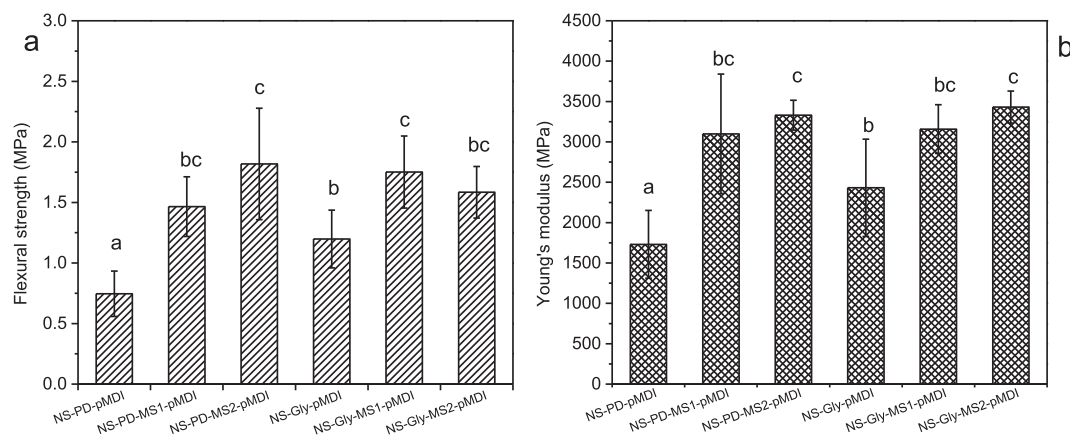


Fig. 6. Flexural bending strength (a) and Young's modulus (b) of PU films. The indicators were statistically tested with ANOVA and Tukey's HSD test at an error probability of $\alpha = 0.05$, $n = 5$.

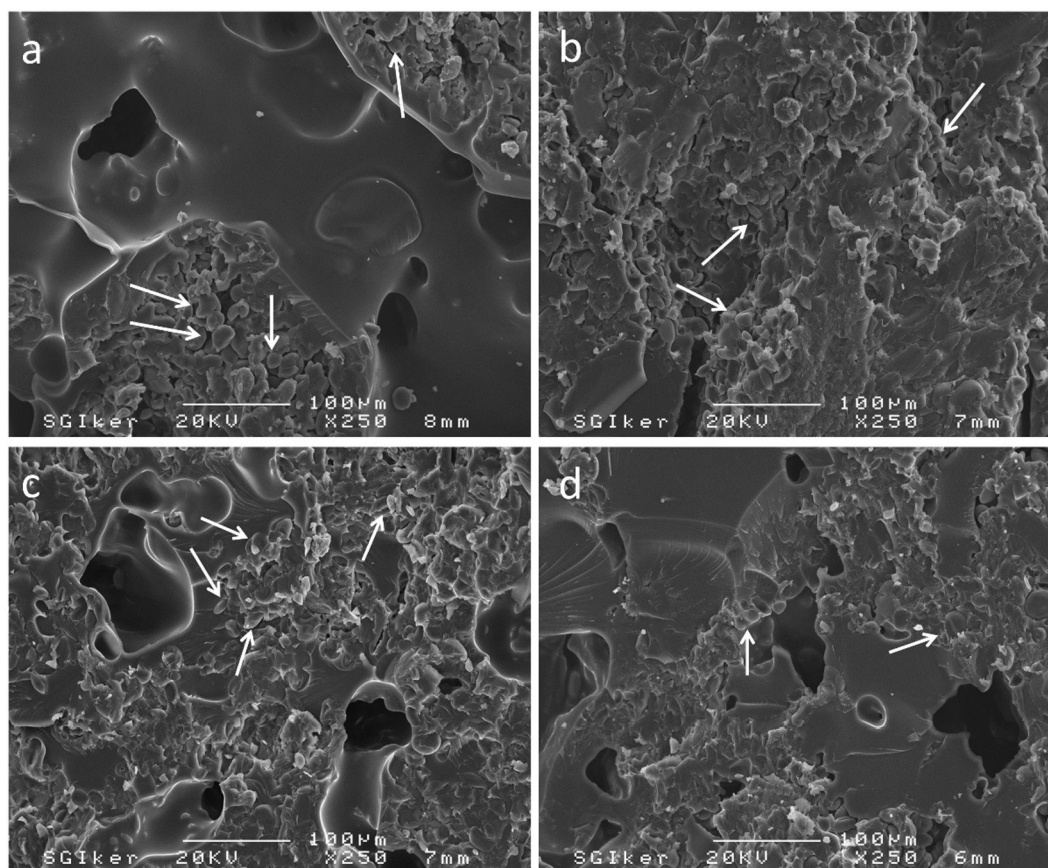


Fig. 7. SEM micrographs from fractured surfaces of PU films after the bending tests. a) NS-PD-pMDI, b) NS-PD-MS2-pMDI, c) NS-Gly-pMDI, and d) NS-Gly-MS2-pMDI. White arrows indicate NS granules.

Formal analysis, Investigation, Data curation, Writing – original draft, Visualization. **Stergios Adamopoulos:** Funding acquisition, Writing – review & editing. **Arantzazu Santamaria Echart:** Investigation, Data curation, Writing – review & editing. **Arantxa Eceiza:** Conceptualization, Writing – review & editing.

Declaration of Competing Interest

The authors declare that they have no known competing financial interests or personal relationships that could have appeared to influence the work reported in this paper.

Acknowledgements

The authors acknowledge the financial support of Lantmännen Forskningsstiftelse (Grant No. 2017H011), University of the Basque Country (UPV/EHU) (GIU18/216 Research Group) and Basque Government (PIBA2020-1-0041). Authors are also grateful to the SG Iker units of the UPV/EHU. Dr Hosseinpourpia also wishes to thank the support of Formas, Swedish Research Council for Sustainable Development (Future research leaders, Grant No. 2018-00637).

Appendix A. Supplementary material

Supplementary data to this article can be found online at <https://doi.org/10.1016/j.eurpolymj.2021.110826>.

References

- [1] N. Girouard, S. Xu, G. Schueneman, M. Shofner, J. Meredith, Site-selective modification of cellulose nanocrystals with isophorone diisocyanate and formation

- of polyurethane-CNC composites, *ACS Appl Mater Inter.* 8 (2016) 1458–1467, <https://doi.org/10.1021/acsami.5b10723>.
- [2] A. Solanki, M. Das, S. Thakore, A review on carbohydrate embedded polyurethanes: An emerging area in the scope of biomedical applications, *Carbohydr Polym.* 181 (2018) 1003–1016. <https://doi-org.proxy.lnu.se/10.1016/j.carbpol.2017.11.049>.
- [3] M. Ilavsk, H. Ulmer, K. Te Nijenhuis, W. Mijs, Network formation in polyurethanes based on triisocyanate and diethanolamine derivatives, *Eur. Polym. J.* 37 (2001) 887–896. [https://doi-org.proxy.lnu.se/10.1016/S0014-3057\(00\)00217-2](https://doi-org.proxy.lnu.se/10.1016/S0014-3057(00)00217-2).
- [4] J. Konieczny, K. Loos, Bio-based polyurethane films using white dextrans, *J. Appl. Polym. Sci.* 136 (2019) 47454. <https://doi-org.proxy.lnu.se/10.1002/app.47454>.
- [5] J. Bernardini, P. Cinelli, I. Anguillesi, M. Coltelli, A. Lazzari, Flexible polyurethane foams green production employing lignin or oxypropylated lignin, *Eur. Polym. J.* 64 (2015) 147–156. <https://doi-org.proxy.lnu.se/10.1016/j.eurpolymj.2014.11.039>.
- [6] S. Chuayjuljit, A. Maungchareon, O. Saravari, Preparation and properties of palm oil-based rigid polyurethane nanocomposite foams, *J. Reinf. Plast. Compos.* 29 (2010) 218–225. <https://doi-org.proxy.lnu.se/10.1177/0731684408096949>.
- [7] L. Rueda, B. Fernández d'Arlas, Q. Zhou, L.A. Berglund, M.A. Corcuera, I. Mondragon, A. Eceiza, Isocyanate-rich cellulose nanocrystals and their selective insertion in elastomeric polyurethane, *Compos Sci Technol.* 71 (2011) 1953–1960. <https://doi-org.proxy.lnu.se/10.1016/j.compscitech.2011.09.014>.
- [8] A.C.W. Tan, B.J. Polo-Cambrenell, E. Provaggi, C. Ardila-Suarez, G.E. Ramirez-Caballero, V.G. Baldovino-Medrano, D.M. Kalaskar, Design and development of low cost polyurethane biopolymer based on castor oil and glycerol for biomedical applications, *Biopolymers.* 109 (2018) 23078. <https://doi-org.proxy.lnu.se/10.1002/bip.23078>.
- [9] A. Gandini, Polymers from renewable resources: a challenge for the future of macromolecular materials, *Macromolecules* 41 (2008) 9491–9504, <https://doi.org/10.1021/ma801735u>.
- [10] N. Masina, Y.E. Choonara, P. Kumar, L.C. du Toit, M. Govender, S. Indermun, A review of the chemical modification techniques of starch, *Carbohydr Polym.* 157 (2017) 1226–1236. <https://doi-org.proxy.lnu.se/10.1016/j.carbpol.2016.09.094>.
- [11] A.L. Da Róza, A.S. Curvelo, A. Gandini, Preparation and characterization of crosslinked starch polyurethanes, *Carbohydr Polym.* 77 (2009) 526–529. <https://doi-org.proxy.lnu.se/10.1016/j.carbpol.2009.01.035>.
- [12] A.C. Brown, *Understanding food: Principles and preparation, fifth ed.*, Cengage Learning, Boston, 2014.

- [13] F. Zia, K. Zia, M. Zuber, S. Kamal, N. Aslam, Starch based polyurethanes: A critical review updating recent literature, *Carbohydr. Polym.* 134 (2015) 784–798. <https://doi-org.proxy.lnu.se/10.1016/j.carbpol.2015.08.034>.
- [14] J. Zou, F. Zhang, J. Huang, P.R. Chang, Z. Su, J. Yu, Effects of starch nanocrystals on structure and properties of waterborne polyurethane-based composites, *Carbohydr. Polym.* 85 (2011) 824–831. <https://doi-org.proxy.lnu.se/10.1016/j.carbpol.2011.04.006>.
- [15] N.L. Tai, R. Adhikari, R. Shanks, B. Adhikari, Flexible starch-polyurethane films: Physicochemical characteristics and hydrophobicity, *Carbohydr. Polym.* 163 (2017) 236–246. <https://doi-org.proxy.lnu.se/10.1016/j.carbpol.2018.06.019>.
- [16] A.R. Solanki, B.V. Kamath, S. Thakore, Carbohydrate crosslinked biocompatible polyurethanes: Synthesis, characterization, and drug delivery studies, *J. Appl. Polym. Sci.* 132 (2015) 42223. <https://doi-org.proxy.lnu.se/10.1002/app.42223>.
- [17] M. Valodkar, S. Thakore, Isocyanate crosslinked reactive starch nanoparticles for thermo-responsive conducting applications, *Carbohydr. Res.* 345 (2010) 2354–2360. <https://doi.org/10.1016/j.carres.2010.08.008>.
- [18] R. Santayanon, J. Wootthikanokkhan, Modification of cassava starch by using propionic anhydride and properties of the starch-blended polyester polyurethane, *Carbohydr. Polym.* 51 (2003) 17–24. [https://doi.org/10.1016/S0144-8617\(02\)00109-1](https://doi.org/10.1016/S0144-8617(02)00109-1).
- [19] R. Hosseinpourpia, A. Echart, S. Adamopoulos, N. Gabilondo, A. Eceiza, Modification of pea starch and dextrin polymers with isocyanate functional groups, *Polymers*. 10 (2018) 939. <https://doi.org/10.3390/polym10090939>.
- [20] R. Hosseinpourpia, S. Adamopoulos, C. Mai, Tensile strength of handsheets from recovered fibers treated with N-methylol melamine and 1,3-dimethylol-4,5-dihydroxyethyleneurea, *J. Appl. Polym. Sci.* 132 (2015) 41290. <https://doi.org/10.1002/app.41290>.
- [21] Q. Liu, J. Li, W. Xu, Application of Cationic Starch with High Degree of Substitution in Packaging Paper from High Yield Pulp. 17th IAPRI World Conf. Packag., 2010, pp. 35–38, 978-1-935068-36-5.
- [22] S. Garg, A.K. Jana, Characterization and evaluation of acylated starch with different acyl groups and degrees of substitution, *Carbohydr. Polym.* 83 (2011) 1623–1630. <https://doi-org.proxy.lnu.se/10.1016/j.carbpol.2010.10.015>.
- [23] R. Colussi, V. Pinto, S. El Halal, N. Vanier, F. Villanova, M. Silva, E. da Rosa Zavareze, A. Dias, Structural, morphological, and physicochemical properties of acetylated high-, medium-, and low-amylose rice, *Carbohydr. Polym.* 103 (2014) 405–413. <https://doi-org.proxy.lnu.se/10.1016/j.carbpol.2013.12.070>.
- [24] H. Tang, B. Hills, Use of ^{13}C MAS NMR to study domain structure and dynamics of polysaccharides in the native starch granules, *Biomacromolecules* 4 (2003) 1269–1276. <https://doi.org/10.1021/bm0340772>.
- [25] H. Garcia, A.S. Barros, C. Goncalves, F.M. Gama, A.M. Gil, Characterization of dextrin hydrogels by FTIR spectroscopy and solid state NMR spectroscopy, *Eur. Polym. J.* 44 (2008) 2318–2329. <https://doi-org.proxy.lnu.se/10.1016/j.eurpolymj.2008.05.013>.
- [26] S. Gómez-Fernández, L. Ugarte, T. Calvo-Correas, C. Pena-Rodríguez, M. Corcuera, A. Eceiza, Properties of flexible polyurethane foams containing isocyanate functionalized kraft lignin, *Ind. Crops. Prod.* 100 (2017) 51–64. <https://doi-org.proxy.lnu.se/10.1016/j.indcrop.2017.02.005>.
- [27] M. Marschner, W. Ritter, ^{13}C NMR studies on the relative reactivity of isocyanate groups of isophorone diisocyanate isomers, *Macromol. Chem. Phys.* 191 (1990) 1843–1852. <https://doi-org.proxy.lnu.se/10.1002/macp.1990.021910810>.
- [28] X. Liu, Y. Wang, L. Yu, Z. Tong, L. Chen, H. Liu, X. Li, Thermal degradation and stability of starch under different processing conditions, *Starke*. 65 (2013) 48–60. <https://doi-org.proxy.lnu.se/10.1002/star.201200198>.
- [29] M. Barikani, M. Mohammadi, Synthesis and characterization of starch-modified polyurethane, *Carbohydr. Polym.* 68 (2007) 773–780. <https://doi-org.proxy.lnu.se/10.1016/j.carbpol.2006.08.017>.
- [30] A. Hejna, Kirpluks, M.P. Kosmela, U. Cabulis, J. Haponiuk, Ł. Piszczczyk, The influence of crude glycerol and castor oil based polyol on the structure and performance of rigid polyurethane-polyisocyanurate foams, *Ind. Crops. Prod.* 95 (2017) 113–125. <https://doi-org.proxy.lnu.se/10.1016/j.indcrop.2016.10.023>.
- [31] A. Saralegi, L. Rueda, L. Martin, A. Arbelaz, A. Eceiza, A. Corcuera, From elastomeric to rigid polyurethane/cellulose nanocrystal bionanocomposites, *Compos. Sci. Technol.* 88 (2013) 39–47. <https://doi.org/10.1016/j.compscitech.2013.08.025>.
- [32] T. Calvo-Correas, M. Mosiewicki, M. Corcuera, A. Eceiza, M. Aranguren, Linseed oil-based polyurethane rigid foams: synthesis and characterization, *J. Renew. Mater.* 3 (2015) 3–13. <https://doi.org/10.7569/JRM.2014.634132>.
- [33] T. Gruke, New Advanced in Polymeric MDI Variants, EUROCOAT 2002, Barcelona, <http://docplayer.net/20924200-New-advances-in-polymeric-mdi-variants.html>.
- [34] T. Gaaz, A. Sulong, M. Ansari, A. Kadhum, A. Al-Amiery, M. Nassir, Effect of starch loading on the thermo-mechanical and morphological properties of polyurethane composites, *Materials*. 10 (2017) 777. <https://doi.org/10.3390/ma10070777>.